

Anti-Human Embryonic Stem Cell Monoclonal Antibody Hesca-2 Binds to a Glycan Epitope Commonly Found on Carcinomas

Mohamed G. Shoreibah,¹ Crystal L. Jackson,¹ Paul W. Price,¹ Richard Meagher,²
Andrew K. Godwin,³ Qi Cai,³ and Jeffrey C. Gildersleeve⁴

Hesca-2, a monoclonal antibody (mAb) IgM raised to the human embryonic stem cell (hESC) line BG-01v, binds with high affinity (nM) to the disaccharide epitope (Gal β 1-3GlcNAc) on a glycan microarray. This epitope was expressed on pluripotent progenitor hESCs in culture, but not in various differentiated cells derived from hESC based on immunofluorescence microscopy. Hesca-2 stains a limited subset of cells in adult human tissues (eg, esophagus and breast). This mAb also crossreacts in immunofluorescence microscopy studies with several human ovarian cancer cell lines and is cytotoxic to them based on the release of cytosolic enzyme lactate dehydrogenase into the media. Hesca-2 immunohistochemically stained tissue from a number of human tumors, including ovary, breast, colon, and esophageal cancer. These data suggest that Hesca-2 recognizes a surface marker found both in stem cells and certain cancer cells.

Introduction

TRACKING THE PHENOTYPIC CHANGES that occur during human embryonic stem cell (hESC) differentiation is vital to their use in regenerative medicine. These changes include differences in the level of expression of cell surface molecules, which can be used as markers. Detection of hESC markers with monoclonal antibodies (mAbs) is the most common method used to confirm their pluripotent progenitor status. Among the limited number of cell surface markers that are used to demonstrate the undifferentiated, pluripotent status of human stem cell populations are the glycoproteins TRA-1-60, TRA-1-81, and the glycolipids SSEA-4 and SSEA-3 [1–5]. Further, other cell surface glycoconjugates are used to define differentiated lineages. CD34 is used to identify and isolate hematopoietic progenitor cells [6,7]. CD133 and polysialylated neural cell adhesion molecule are used to delineate neural stem cells. In addition, CD133 is a stem cell surface glycoprotein that has been shown to be cancer stem cell marker [8–10]. Polysialylated neural cell adhesion molecule is a cell-surface glycan marker that is developmentally regulated containing a linear homopolymer composed of α 2-8-linked sialic acids. The glycan polysialic acid has a functional role in axonal growth and synaptogenesis and has been shown to act as a repulsive signal on immature neurons [11,12].

Although antibodies against cell surface glycoconjugates have proven valuable for studies on hESC, new antibodies

for tracking changes during hESC differentiation are needed. One of the primary challenges for obtaining new hESC antibodies is the lack of molecularly defined target antigens. An alternative approach we have taken involves immunization with whole hESCs, followed by screening of the resulting hybridomas to identify mAbs with the appropriate characteristics. Using this strategy, antigen targets do not need to be known beforehand to obtain useful antibodies and one can potentially identify novel hESC antigens. In addition, the whole-cell immunization strategy results in an enrichment of antibodies to cell surface antigens.

In a collaborative project with Viacyte (formerly, BresaGen) we have generated a number of anti-hESC mAbs to the hESC line BG-01v (NIH registry) [13]. In this study, we describe the characterization of one of these mAbs, Hesca-2, which stains novel cell surface antigen(s) on undifferentiated progenitor cells. We demonstrate with immunofluorescent staining that Hesca-2 selectively stains hESCs but not mouse ESCs (mESCs) or differentiated feeder cells. We also show that Hesca-2 binds to human ovarian cancer cell lines and is cytotoxic to them. In addition, immunohistochemistry with the antibody shows staining of various common tumor types on tissue microarrays (TMAs) from patient samples, including esophageal, breast, colon, and ovarian carcinomas. Finally, using a glycan microarray, we report that Hesca-2 recognizes, with high apparent affinity, glycan epitopes containing the Lewis C (LeC; also referred to as the type 1

¹Abeome Corporation, Athens, Georgia.

²Department of Genetics, University of Georgia, Athens, Georgia.

³Fox Chase Cancer Center, Philadelphia, Pennsylvania.

⁴National Cancer Institute, Frederick, Maryland.

precursor) disaccharide, Gal β 1-3GlcNAc. Thus, this study demonstrates that this disaccharide, observed on a number of carcinomas, is also present on the cell surface of hESCs and on limited set of adult tissues. Therefore, Hesca-2 recognizes a glycan that may be a novel cancer stem cell surface marker.

Materials and Methods

Chemicals and reagents

Unless otherwise noted all chemicals were purchased from Sigma and were reagent grade. Hesca-2 mAb was purified at Abeome with a combination of ammonium sulfate precipitation, ceramic hydroxyapatite (type II; BioRad) chromatography, and cation exchange chromatography on HiTrap SP FF (GE Healthcare) cartridges. Hesca-2 was also obtained from Millipore Corporation.

Cell lines

The following cell line were used in this study: BG-01v, BG02, mESCs, and murine embryonic fibroblasts were provided by Viacyte; OVCAR3, CaOV3, SKOV3, and HS-27 were purchased from ATCC; BG-1 was obtained from the D. Puett Laboratory (University of Georgia, Athens, GA). The Hesca-2 hybridoma cell line was isolated and characterized at Abeome Corporation as described below. All cells were maintained in defined media in humidified incubators at 37°C. Formation of teratomas from embryonic cells for use in this study was made as previously described [14].

Generation of antibodies

Cultured BG-01v cells were verified for expression of Oct-4 and SSEA-3, -4 (not shown), and harvested using enzyme-free cell dissociation buffer (Invitrogen). All studies involving animals obtained IACUC approval from the University of Georgia, School of Veterinary Medicine, where the work was done. Mice were immunized intraperitoneally with $\sim 10^8$ fixed cells in phosphate-buffered saline (PBS), boosts of $\sim 10^7$ cells/per mouse at 30-day intervals, and $\sim 10^6$ cells given 3–4 days before harvest. Mice that demonstrated serum antibody titers of $\geq 1:3,000$ in whole-cell ELISAs were sacrificed and splenectomized. Splenocytes were fused with Abeome's SP2ab myeloma cells (described below) using polyethylene glycol and cultured in Iscove's modified Dulbecco's media containing 20% fetal bovine serum under hypoxanthine, aminopterin, and thymidine (Sigma-Aldrich) [15] selection.

Antibody secreting hybridoma cell lines were isolated by fluorescent-activated cell sorting (FACS) based on expression of the membrane isovariant of that antibody in the B cell antigen receptor (BCR) complex on the cell surface using a proprietary process described previously [16]. Briefly, this process relies on fusing splenocytes with a myeloma (SP2ab) that has been genetically engineered to constitutively express the Ig α and Ig β (CD79a and CD79b) components of the BCR. Hybridomas generated with SP2ab demonstrate consistent expression of the BCR on their cell surface in addition to secreting antibody. Thus, hybridomas can be rapidly selected with fluorescently labeled antigens, and, using FACS, deposited singly into wells of a 96-well culture plate.

Plasma membrane antigen (PMA) fractions were prepared for labeling by conjugating live, un-fixed, intact BG-01v cells with biotin, followed by 10 min fixation in 0.4% paraformaldehyde, and ultrasonic disruption. Hybridomas were removed from culture, washed, labeled with biotin-conjugated PMA fractions, and counterstained with streptavidin-conjugated r-phycoerythrin (BD Biosciences) and allophycocyanin-conjugated goat anti-mouse Ig (Invitrogen). Sorting was done using a FACS Aria™ Flow Cytometer (BD Biosciences) as described previously [16]. Cells positive for both Ig expression and PMA reactivity were deposited singly into 96-well culture plates containing Iscove's modified Dulbecco's media supplemented with 20% fetal bovine serum, hypoxanthine, and thymidine (Sigma-Aldrich). The isotype of each clone was determined by ELISA using the Zymed MonoAb isotyping kit (Invitrogen).

Immunofluorescence microscopy

Immunofluorescent staining of BG-01v and other cells with Hesca-2 was performed using standard immunofluorescence microscopy (IFM) techniques as described previously. Briefly, 1×10^5 cells were cultured in 4-well chamber slide cultures (Lab-Tek Permanox Chamber slides; Nalge Nunc Int.) for 48 h. Cells were then fixed for 10 min with 4% paraformaldehyde, blocked with 10% goat serum in PBS, and probed with culture supernatants diluted 1:10 in 1% goat serum or when using purified antibody diluted to 10 μ g/mL in PBS. Cells were stained with FITC-conjugated goat anti-mouse IgG+IgM (Sigma) diluted 1:50 in 1% goat serum in PBS, and counterstained with DAPI. Images were observed and photographed on a Leica DM RXA fluorescence microscope.

Effect of Hesca-2 on cells in culture

Cytotoxicity of Hesca-2 toward the ovarian cancer cell lines SKOV3 and OVCAR3 in culture was assayed by measuring the release of the lactate dehydrogenase (LDH) into the culture media from dead or dying cells. After incubation of the mAb at a concentration of 0.02, 0.2, 2, and/or 20 μ g/mL on the cells for 48 h, we measured the level of LDH enzyme in culture supernatants. For these enzyme assays we utilized a colorimetric kit from BioVision which yields a product detected at 450 nm following the manufacturer's protocol. Enzyme assays were done in triplicate and values averaged. To assess whether the cytotoxicity observed with Hesca-2 could be due to induction of apoptosis in the ovarian cancer cells, we utilized an M30-Apoptosense ELISA (Peviva AB), which measures a neopeptide generated following cleavage of cytokeratin-18 by activated caspases.

For the hESC line BG-02 cell growth/death in the presence of Hesca-2 was monitored using both LDH release and a xCELLigence real-time cell analyzer (Roche). This instrument measures impedance across the bottom of a specialized microtiter plate which is affected by cell number, morphology, adherence, and viability. BG02 cells were plated in StemPro hESC SFM media (Invitrogen; Cat. No. A1000701) at a density of 20×10^3 cells per well in microelectronic sensor array integrated-96-well plates coated with Matrigel (BD Biosciences; Cat. No. 356231) and allowed to adhere for 25 h. After 25 h, the medium was removed and replaced with

medium containing 0.02, 2.0, 10, or 20 mg/mL of anti-hESC mAb HESCA-2. The negative control was media alone. Treatments were applied in quadruplicate and monitored in real time. Impedance was measured from the time of seeding to 72 h after HESCA-2 treatment. LDH assays were performed as described above on conditioned medium aliquots taken at 24 and 48 h after antibody addition and the results averaged after subtracting the absorbance due to media alone.

Immunohistochemistry

Using standard immunohistochemical methodology, patient TMAs prepared at the Fox Chase Cancer Center Biosample repository were stained with HESCA-2. Briefly, fixed paraffin-embedded tissue sections were immunoperoxidase labeled after antigen retrieval. Deparaffinization of the slides was done using an automated DAKO instrument. Endogenous peroxidase activity was inactivated by a 5–10 min incubation in 3% H₂O₂ in distilled water. Antigen retrieval, which is antigen-dependent process, was accomplished with a 10 min incubation at 120°C in a DAKO cytomation pressure cooker. After rinsing the array slides in PBS for 5 min, they were blocked with normal goat serum for 20 min at room temperature (RT). We then applied the primary antibody, at a 1:500 dilution (of a 0.9 mg/mL stock) for an hour at RT. After again rinsing the array slides in PBS for 5 min, we incubated the slides with a biotin-conjugated anti-mouse secondary antibody at 20°C–37°C for 20 min. The SABC reagent (Vector Labs) is added to the slides at 37°C for 20 min. After rinsing the array slides several times chromogen development with diaminobenzidine (DAB) proceeded until the desired degree of staining was achieved. Finally, the slides were stained with hematoxylin (Gil II, SurgiPath) and mounted (Cytoseal).

SDS-PAGE and western blot analysis

Electrophoresis was performed in a discontinuous buffer system on precast 10% (w/v) polyacrylamide gels (BioRad; Cat. No. 161-1101). BG-01v cell pellet was mixed with 2 × sample buffer (4% SDS, 0.2% bromphenol blue, 100 mM dithiothreitol, and 20% glycerol in 100 mM Tris-buffered saline), boiled for 5 min, and electrophoresed. Separated proteins were electroblotted onto polyvinylidene difluoride membranes (Immobilon P) using a semidry blot apparatus (Biorad) set at 11 mAmp for 80 min using transfer buffer [20% (v/v) methanol, 48 mM Tris, 39 mM glycine (pH 9.2), 0.04% SDS]. Before transfer, the membrane was soaked in methanol for 1 min, and the membrane and the gel were incubated in transfer buffer for 10 min. After transfer, the membrane was blocked for overnight at 4°C in 3% bovine serum albumin [BSA] in TBST buffer [20 mM Tris-HCl (pH 7.6), 140 mM NaCl, and 0.1% Tween 20]. Before addition of the primary antibody, the blot was rinsed briefly with TBST buffer and incubated with HESCA-2 antibody (1 mg/mL) for 1 h at RT. After 3 washes with TBST the blot was incubated for 30 min with a polyclonal rabbit anti-mouse antibody conjugated to HRP diluted 1:2,000 (DakoCytomation). The membrane was then washed 3 times with TBST buffer and incubated with ECL substrate (Pierce; product 32106) following manufacturer's instructions and exposed to film (Biomax MR; Kodak).

Glycan microarray

Carbohydrate microarrays were fabricated as reported previously [17–19]. Briefly, each array component was printed in duplicate within a 20 × 20 grid of 110 μm diameter spots. Each slide was printed with 16 complete grids/arrays. A description of the 204 array components is given in Supplementary Table S1 (Supplementary Data are available online at www.liebertonline.com/scd). Printed slides were stored at –20°C until used. The 16-well slide modules/holders (Grace Bio-Labs) were then assembled on the printed slides and wells were blocked with 3% BSA (w/v) in PBS for 2 h at RT. Purified HESCA-2 was diluted to various concentrations ranging from 0.01 to 29 μg/mL in 3% BSA in PBS to produce a dilution series. Each dilution was incubated in a separate well on the slide (75 μL/well) for 2 h at RT. Each concentration/dilution was analyzed in quadruplicate. After washing with PBS, bound antibody was detected by incubating with Cy3-conjugated goat anti-mouse Ig (Jackson ImmunoResearch) diluted to 2 μg/mL in 3% BSA/PBS for 1 h at RT. Wells were washed with PBS 4 times, and then the 16 well module was removed. Slides were immersed in PBS buffer 3 times for 2 min, and then centrifuged at 453 g for 5 min. Slides were scanned at 10 μm resolution with a Genepix 4000B microarray scanner (Molecular Devices Corporation) with a photomultiplier tube (PMT) setting such that no saturated pixels were obtained. Images were analyzed with Genepix Pro 6.0 analysis software (Molecular Devices Corporation). Spots were defined as circular features with a maximum diameter of 100 μm. Features were allowed to be resized down to 70 μm as needed. Local background subtraction (median background) was performed. Initial data processing was performed with Microsoft Excel. To obtain a single relative fluorescence units (RFU) value for each array component at a given HESCA-2 concentration, the mean of the 8 spots (4 wells × 2 replicate spots) was used. Apparent dissociation constants (K_ds) were determined using Origin 8 software (OriginLab).

Results

Immunofluorescence on hESCs, mESCs, and differentiated cells

IFM was used to discern the staining pattern of HESCA-2 on hESCs, mESCs, and the various feeder cells used in culturing embryonic stem cells. Figure 1 shows the global pattern of cell staining obtained with HESCA-2 on hESC line BG-02. The strong wide-spread staining suggests an abundance of the antigen(s) on nearly all cells, the high affinity of the mAb to its target antigen, or some combination of both factors. By contrast, there was little staining to mESCs and no staining to Hs-27 or murine embryonic fibroblasts, which are commonly used as feeder cells for stem cell culture (not shown) by HESCA-2. Teratomas derived from BG02 hESCs displayed rare positive staining (not shown).

HESCA-2 stains and is cytotoxic to OC cells

In addition to staining of stem cell lines, we assayed, by IFM, for the presence of HESCA-2 reactive antigen(s) on the human epithelial ovarian cancer lines BG-1, OVCAR3, SKOV3, and CaOV3. There was weak staining on these cells by HESCA-2 (not shown). When SKOV3 cells were cultured

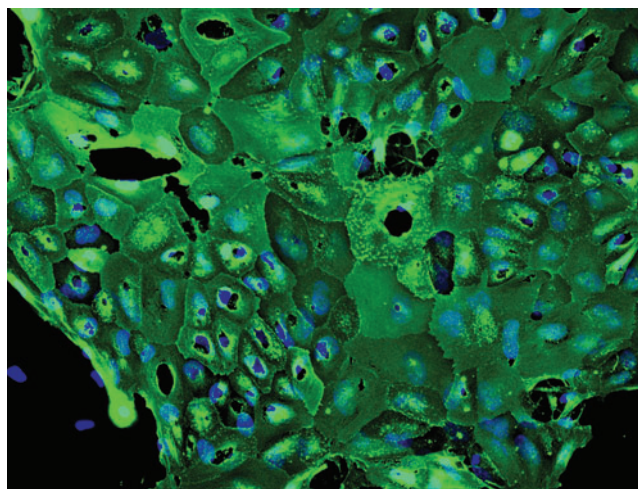


FIG. 1. Immunofluorescent staining by Hesca-2 on BG-02 hESCs cultured in LabTek chamber slides. Slides were stained with Hesca-2 and counterstained with goat anti-mouse Ig conjugated to FITC (green). Nuclear staining appears blue (DAPI); 20 \times magnification. hESCs, human embryonic stem cells.

in the presence of the 0.02–20 $\mu\text{g}/\text{mL}$ of antibody for 48 h, cytotoxicity of up to 20% was detected as measured by LDH release as shown in Fig. 2. Unexpectedly, cell killing was maximal at 2 $\mu\text{g}/\text{mL}$ and less at the higher concentration (20 $\mu\text{g}/\text{mL}$) of antibody. Cytotoxicity was much less evident in OVCAR3 cells treated over the same range of Hesca-2.

By contrast to the cytotoxicity observed with intact antibody, Fab fragment generated from Hesca-2 had no significant effect at 0.4 and 40 $\mu\text{g}/\text{mL}$. The cytotoxic effect was not complement-dependent lysis in that the cells were cultured in heat-inactivated serum. To define the mechanism of this observed cytotoxicity, we tested whether Hesca-2 triggered apoptosis in OVCAR3 and SKOV3 cells. The results showed that apoptosis was not caused by exposure to 20 $\mu\text{g}/\text{mL}$ of Hesca-2 over a 48-h incubation.

We also examined the effect of Hesca-2 on hESCs in culture. Those experiments show a small but reproducible cytotoxic effect at low concentration (0.02 $\mu\text{g}/\text{mL}$) and a more significant cytoprotective/proliferative effect at higher concentrations (>10 $\mu\text{g}/\text{mL}$) as measured by LDH release as shown in Fig. 2. Cell growth was also monitored by a xCELLigence system, which measures electrical impedance across interdigitated microelectrodes integrated into specialized 96-well plates. The cell index (a dimensionless parameter proportional to cell density, viability, and morphology/adhesion) monitored in real time over a 72-h period and depicted in Fig. 3 corroborates the LDH data. As shown in Fig. 3, the untreated and treated cells are indistinguishable until antibody addition at about 25 h. Thereafter, the cells treated with Hesca-2 diverge from untreated cells and demonstrate a dramatic dose-dependent increase in impedance with 10 and 20 $\mu\text{g}/\text{mL}$ of Hesca-2 after 24 h of incubation with antibody when compared to media alone. Treatment with 0.2 and 20 $\mu\text{g}/\text{mL}$ Fab had no significant effect on hESCs (not shown). Similar but not identical trends were seen for the effect of Hesca-2 on BG-02 cells that were

seeded at 1×10^4 and 3×10^4 cells per well densities over the course of 72 h.

Staining on carcinomas versus limited staining of subsets of cells on normal tissues

We examined the immunohistochemical staining of patient tumor tissue on TMAs with Hesca-2. We observed staining on a number of common tumor types as shown in Fig. 4. By contrast, we found limited staining of subsets of cells within normal breast and esophagus but not in normal colon as shown below. The staining, where it was present, was not widespread. A single specimen of each type of tissue was examined except for ovarian cancer where 12 out of 27 samples of serous carcinoma stained with Hesca-2. In most cases the staining displayed an apical pattern or was limited to epithelial cells.

Recognition of high molecular weight species on western blots

The staining of stem cells, ovarian cancer cell lines, and on carcinomas from patient tissue by Hesca-2 heightened our interest in the identity of epitope/antigen(s) targeted by this mAb. Western blot analysis on cell lysate of BG-01v cells, shown below in Fig. 5, revealed a major species migrating at an apparent molecular weight of 250 kDa with a diffuse pattern of staining suggestive of a mucin. Mucins are heavily glycosylated proteins and many antibodies that recognize mucins bind to their carbohydrate moieties. Several less intense bands of lower molecular weights were also observed.

Glycan screening

To ascertain if the antigen recognized by Hesca-2 was a glycan, we screened the antibody on a glycan array. Glycan arrays are analogous to DNA and protein arrays but contain many different oligosaccharides immobilized on a glass microarray slide (for recent reviews, see [20–22]). The glycan array contained a diverse set of 204 carbohydrates and glycoproteins printed on a glass microscope slide using a robotic microarrayer (for a full list of glycans on the array, see supplementary Table S1). This screen demonstrated specific binding to a number of oligosaccharides containing the type 1 chain as seen in Fig. 6, including blood group H1 (BG-H1), lacto-*N*-tetraose (LNT), lacto-*N*-hexaose (LNH), and LeC (also referred to as the type 1 precursor) presented as neoglycoproteins of varying ligand densities. By contrast to the specific binding to these reactive glycans, whose structures are depicted in Fig. 7, >90% of the glycans on the array were non-reactive displaying background RFU values that were between 3 and 4 orders of magnitude lower in intensity (see Supplementary Table S2 for the complete list). On the basis of the binding profile, the minimum glycan epitope is the disaccharide, Gal β 1-3GlcNAc. Several closely related structures, including Gal β 1-3GalNAc and Gal β 1-4GlcNAc, were not recognized by the antibody. Some modifications of the core disaccharide were tolerated. For example, Hesca-2 bound well to BG-H1, which contains a fucose residue alpha linked to the 2 position of the galactose, and LSTc, which contains a sialic acid residue alpha linked to the 6 position of the GlcNAc residue. Other modifications, however, were not tolerated. For example, LSTa (Sia α 2-3Gal β 1-3GlcNAc β 1-3Gal β), LSTc

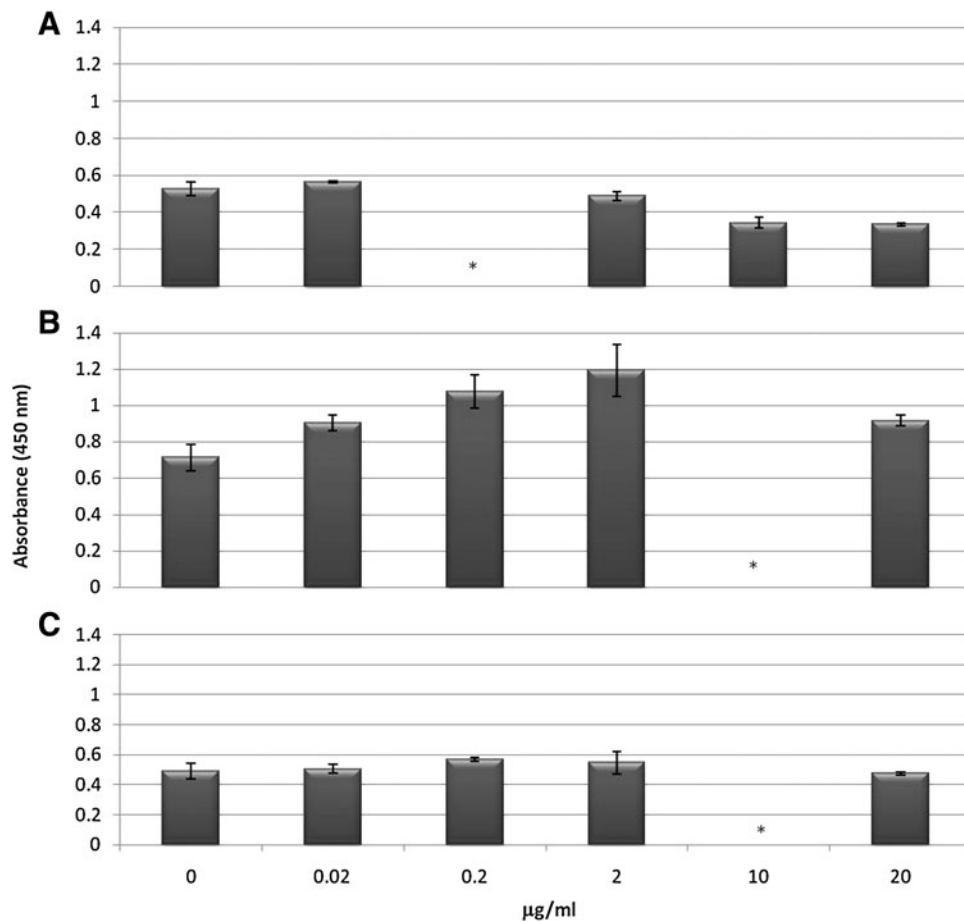


FIG. 2. Effect of HESCA-2 on release of the LDH enzyme on hESCs (A), SKOV-3 (B), or OVCAR-3 (C) cells in culture. Cells were treated for 48 h with increasing concentrations (0.02–20 µg/mL) of HESCA-2 or with media alone. LDH activity was measured using an assay kit that yields a colorimetric product that is detected at OD450 nm. Tests were done in at least triplicate and the results averaged. Standard deviations were computed and are shown as error bars. Comparable results were obtained in 2 independent experiments. *A concentration not tested in the respective experiment. LDH, lactate dehydrogenase.

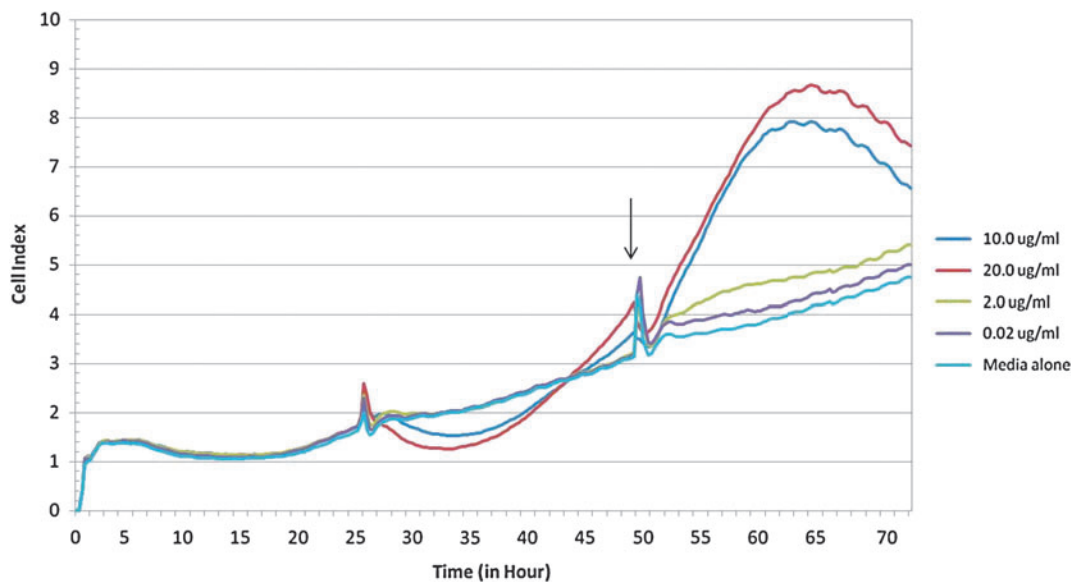


FIG. 3. Impedance analysis, in real-time, of BG02 cells treated with increasing concentrations (0.02–20 µg/mL) of HESCA-2. Data were collected using an xCELLigence analyzer. About 2×10^4 cells were seeded into each well of a microelectronic sensor array integrated-96-well plate. Antibody addition begins at 25 h and fresh media and antibody are added every 24 h thereafter. Arrows indicate time points when the plate was disconnected from the analyzer for cell feeding and to collect aliquots for LDH release analysis. These data are the average of quadruplicate treatments and standard deviations were <0.35, 0.20, 0.37, 1.02, and 1.40 for the 0, 0.02, 0.2, 10, and 20 µg/mL concentrations of HESCA-2, respectively. Similar but not identical trends were seen for the effect of HESCA-2 on cells of 1×10^4 and 3×10^4 seeding densities over the course of 72 h.

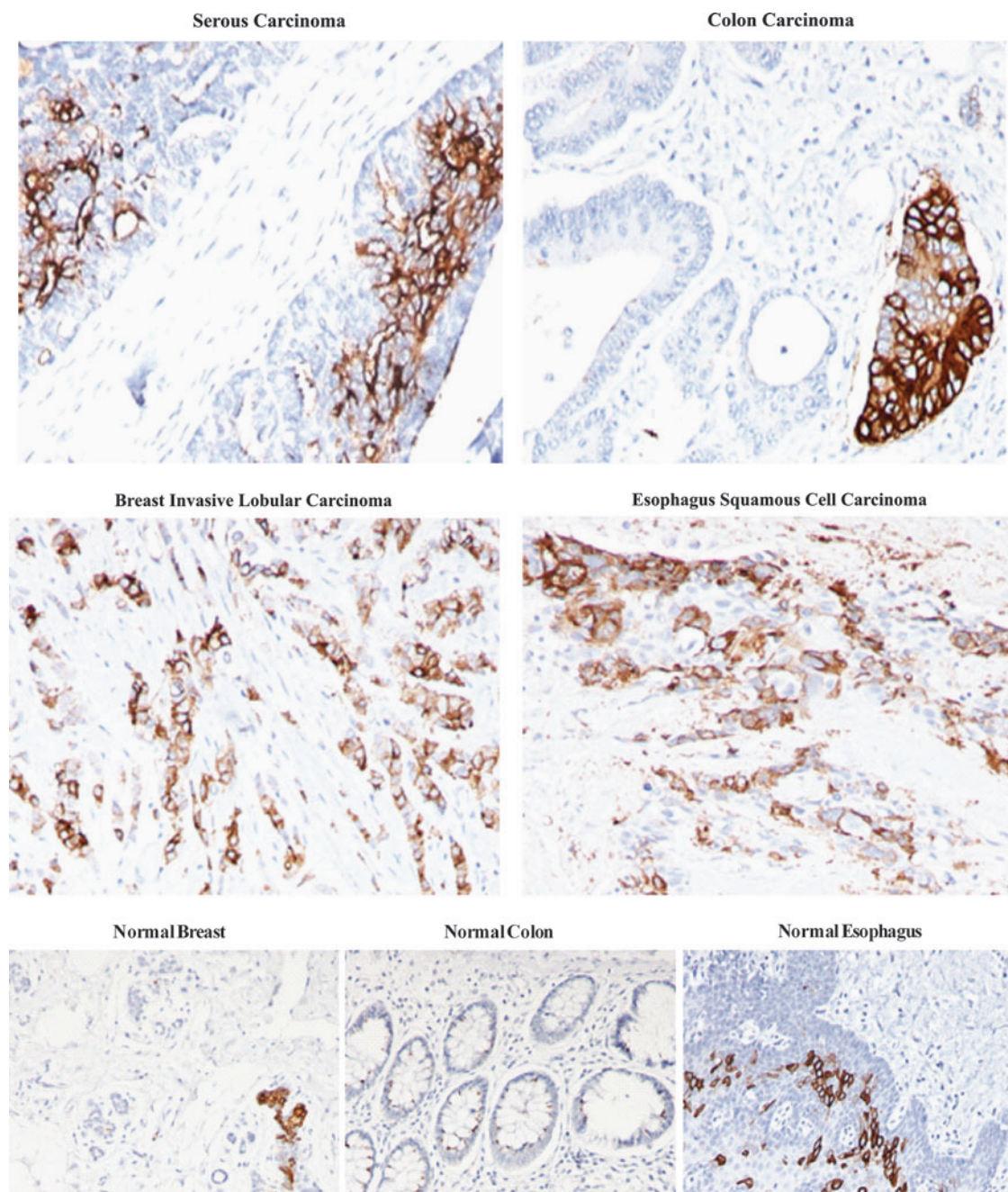


FIG. 4. Immunohistochemical staining of common tumor types and normal tissues. Serous carcinoma, colon carcinoma, breast invasive lobular carcinoma, esophagus squamous cell carcinoma, normal breast, normal colon, and normal esophagus; 20 × magnification.

(Sia α 2-6Gal β 1-3GlcNAc β 1-3Gal β), and Lewis A [LeA; Gal β 1-3[Fuc α 1-4]GlcNAc] were not bound by the antibody.

Determination of apparent affinity for glycans

Apparent dissociation constants were determined in parallel on the glycan array by measuring antibody binding at a range of antibody concentrations following the method of MacBeath [23]. The apparent dissociation constants and maximum signals are listed in Table 1. Hesca-2 bound all 8 oligosaccharides with fairly similar affinity and binding was not substantially affected by variations in carbohydrate

density (eg, LNT-05 vs. LNT-20 and pLNH-07 vs. pLNH-21). Apparent K_ds ranged from 0.30 to 1.86 μ g/mL (0.33–2.07 nM), corresponding to high avidity binding relative to many other carbohydrate binding antibodies.

Discussion

Hesca-2 recognizes the glycan epitope Gal β 1-3GlcNAc

We have demonstrated that Hesca-2 binds to a number of related glycans on a glycan microarray sharing the common

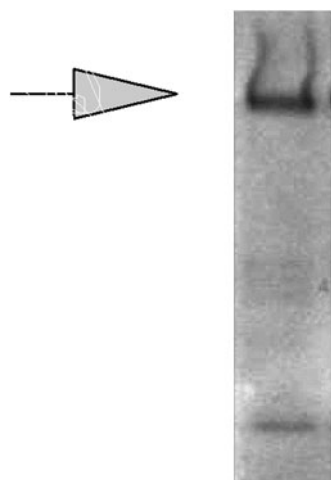


FIG. 5. Western blot on BG-01v cell lysate probed with Hescsa-2 (1:1,000 dilution). Arrow denotes migration of molecular weight marker at 250 kDa.

epitope of [Galβ1-3GlcNAc]. This glycan epitope is found on glycoproteins, glycolipids, and free oligosaccharides in milk [24-26]. It is the precursor sequence for the biosynthesis of type 1 Lewis and blood group antigens, such as BG-A1, BG-B1, BG-H1, LeA, LeB, and SLeA, and it has been referred to as the type 1 precursor and as the LeC antigen.

This glycan epitope is also associated with several human carcinomas, including pancreatic, stomach, colorectal, and ovarian. In fact, a humanized IgG mAb, RAV12, which has similar glycan specificity, has demonstrated *in vivo* antitumor activity against gastrointestinal adenocarcinoma in a mouse xenograft model [27]. RAV12 is also being tested in human clinical trials [28]. In addition to RAV12, there are multiple antibodies with similar specificity as Hescsa-2, including K21 [29], LU-BCRU-G7, FC10.2 [30,31], and F48-60 [32], which are known to bind the type 1 precursor sequence.

Several type 1 precursor-binding mAbs have been isolated from humans, including IgM^{W^{OO}} [33] and HMST-1 [34]. Expression of the glycan epitope has been evaluated using these antibodies in various tissues. As noted above, high levels of expression have been observed with these antibodies on human carcinomas.

Similar to the RAV12 mAb, it is possible that Hescsa-2 is directly cytotoxic to carcinoma-derived cancer cell lines in culture by a dose-dependent mechanism termed oncosis [27]. Oncosis leads to cell death by disruption of cell membranes, ion fluxes, and thereby homeostasis. For both of these antibodies, cytotoxicity requires a multimeric interaction with their glycan ligand as Fab fragments of either mAb are not cytotoxic. This dependence on multimeric binding perhaps accounts for the plateau in cell killing at a 2 mg/mL concentration of Hescsa-2 seen against SKOV3 cells in Fig. 2. We speculate that higher antibody concentration favors more monomeric interactions and therefore the observed reduced cytotoxicity.

We also examined the effect of Hescsa-2 on hESCs in culture. Those experiments show a negligible activity at low concentrations and a dramatic effect on the cells that may be due to cytoprotection or proliferation at higher concentrations of Hescsa-2. The mechanism of this activity clearly requires multimeric binding in that Fab fragments do not show a comparable effect. It is conceivable that Hescsa-2 could be binding 1 glycan (such as LeC) on hESCs and a different glycan (such as BG-H1) on tumor cells, leading to cell type-specific effects. Therefore, identifying the native glycoconjugates recognized on each cell type is important to explore the precise basis of the different cell responses. For example, one could investigate what effect the soluble glycan ligands (recognized by Hescsa-2) have on the proliferation, adhesion, and so forth, of different cell types, including hESCs. On the basis of the western blot data, it is possible that the different cell types share at least 1 common polypeptide backbone, a high molecular weight species, likely a mucin.

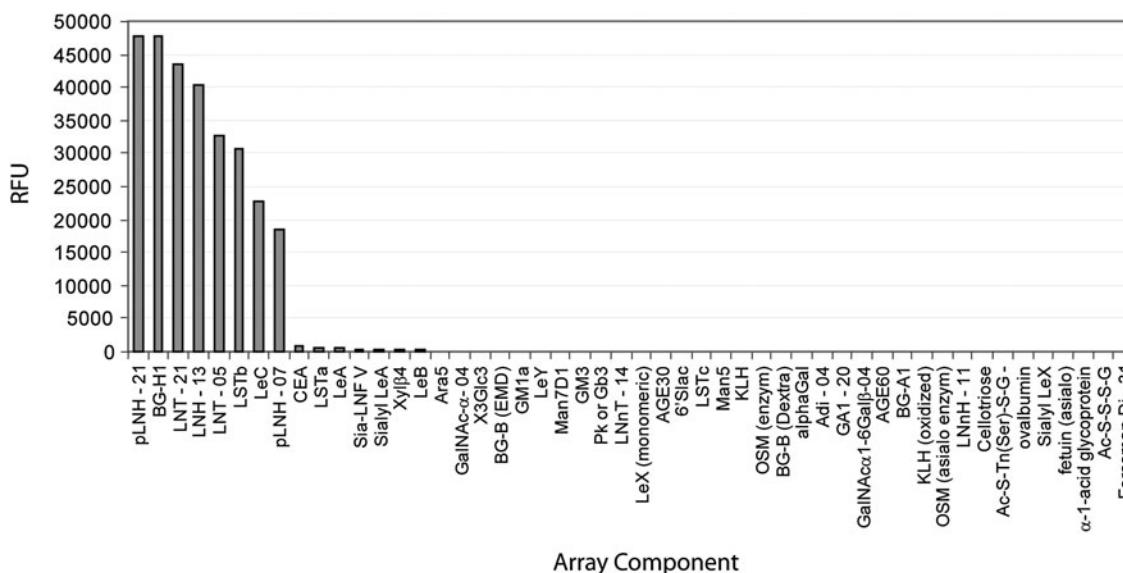


FIG. 6. Glycan array binding results by Hescsa-2.

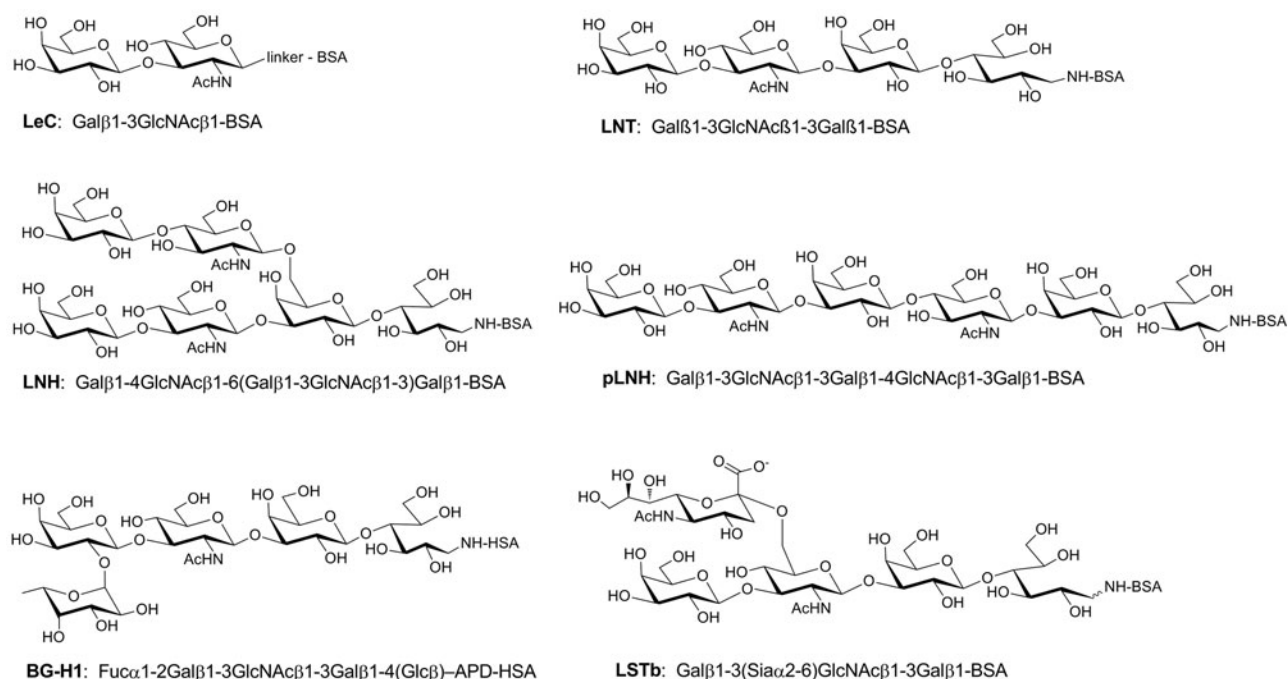


FIG. 7. Glycan structures specifically bound by Hescsa-2.

Glyconjugate epitopes shared by stem cells and cancer cells

Other glycan markers have also been used to identify embryonic as well as mesenchymal (adult) stem cells, such as high-mannose type N-glycans, linear poly-N-acetylglucosamine chains, alpha2-3-sialylation, and sialyl Lewis x epitopes [35–37]. Many of these are also cancer-associated antigens. It is increasingly recognized that stem cells and cancer tissues share common epitopes regardless of the origin of cancer cells [38–42]. CD133 is generally accepted as a marker for mesenchymal progenitor cells. It has been found to be expressed in populations of brain tumor cells, retinoblastomas, ependymoma, prostate cancer, colon cancer, lung cancer, hepatocellular carcinoma, laryngeal carcinoma,

melanoma, ovarian cancer, and pancreatic cancer [41,43,44]. Other markers of stemness, such as CD44⁺ CD24[–], have been found in cells of highly proliferative breast cancer tumors associated with poor prognosis [42,45]. The data presented in this study suggest that the glycan epitope recognized by Hescsa-2 may be another surface marker for cancer stem cells.

Functional role of these glycan epitopes on stem cells—galectins?

The biological roles of the glycans recognized by Hescsa-2 on stem cells, adult cells, or cancer cells are not known. There are a variety of endogenous proteins that could potentially interact with these glycans, and a family of particular interest are galectins. Galectins are carbohydrate-binding proteins that typically recognize galactose containing glycans [46,47], and a number have been shown to bind glycans containing the Gal β 1-3GlcNAc sequence (see Consortium for Functional Glycomics [CFG] website) [48].

The binding properties of galectins have been studied extensively in vitro, and human galectin 7 (hGal7) has the most similar binding to Hescsa-2 [49] (CFG website). It binds well to BG-H1, LeC, LNT, and pLNH; it also binds well to a structure similar to LSTb (but LSTb and LNH were not tested). However, hGal7 also binds LacNAc structures, so it has broader specificity and the glycans responsible for recognition in vivo are not known.

Galectins have been implicated in a wide range of biological processes during development and in adult tissues, including induction of differentiation [50], cell proliferation [51,52], apoptosis [53], cell signaling [54], and adhesion [55,56]. In tumors, galectins have been shown to be involved in cell migration, triggering T-cell apoptosis, adhesion to integrins, and growth promotion [57]. Like other galectins, hGal7 is associated with differentiation and development. It

TABLE 1. MAXIMAL BINDING AND APPARENT K_D TO VARIOUS GLYCANS BY HESCA-2

Name ^a	Max. (RFU)	Apparent K _d (μg/mL)	Apparent K _d (nM)
BG-H1	49,519	0.30	0.33
LNH-13	39,033	0.39	0.43
LNT-20	46,735	0.41	0.46
LNT-05	33,653	0.45	0.50
pLNH-21	49,175	0.50	0.56
LSTb	31,306	0.61	0.68
LeC	21,225	1.11	1.23
pLNH-07	19,239	1.86	2.07

^aThe number after the abbreviation refers to the average number of oligosaccharide chains per molecule of BSA (eg, LNT-20 contains an average of 20 LNT trisaccharide units per BSA).

BSA, bovine serum albumin; LeC, Lewis C; LNH, lacto-N-hexaose; LNT, lacto-N-tetraose.

is involved in the development of pluristratified epithelia and with epithelial cell migration [58]. In addition, in certain tumors it is a regulator of apoptosis.

The mechanism underlying the proliferative and cell signaling effects attributed to galectins has been shown to relate to their clustering of cell surface receptors and the formation of supramolecular lattices [54,59]. It is hypothesized that by binding and crosslinking on the cell surface, in a multivalent fashion, either glycoprotein receptors or transporters, galectins can modulate the signal transduction properties or turnover of these molecules. Whether the disaccharide epitope recognized by Hesca-2 interacts with any of the galectins in vivo or plays a functional role on the cells where it is found remains to be elucidated.

In conclusion, Hesca-2, which stains hESC and numerous carcinomas, binds with high affinity to the disaccharide epitope Gal β 1-3GlcNAc. This glycan can be recognized by a number of human galectins particularly galectin-7. It is highly speculative what the biological function of these glycans may be and the nature of any potential binding partners. There is an intriguing possibility that the glycan ligands recognized by Hesca-2 and galectin-7 (or another galectin) could be involved in processes critical for both stem cell and cancer cell survival or proliferation.

Acknowledgments

This research was supported in part by the Intramural Research Program of the NIH, NCI. The authors would like to thank Dr. Thomas Schulz of ViaCyte for his assistance in developing and characterizing Hesca-2.

Author Disclosure Statement

None of the authors with the exception of Richard Meagher have any commercial associations or competing financial interests that might create or have the potential to create a conflict of interest in connection with this article. Dr. Meagher is a founding scientist, shareholder, and paid consultant to Abeome Corporation.

References

- Henderson JK, JS Draper, HS Baillie, S Fishel, JA Thomson, H Moore and PW Andrews. (2002). Preimplantation human embryos and embryonic stem cells show comparable expression of stage-specific embryonic antigens. *Stem Cells* 20:329–337.
- Carpenter MK, E Rosler and MS Rao. (2003). Characterization and differentiation of human embryonic stem cells. *Cloning Stem Cells* 5:79–88.
- Zeng X, T Miura, Y Luo, B Bhattacharya, B Condie, J Chen, I Ginis, I Lyons, J Mejido, RK Puri, MS Rao and WJ Freed. (2004). Properties of pluripotent human embryonic stem cells BG01 and BG02. *Stem Cells* 22:292–312.
- Badcock G, C Pigott, J Goepel and PW Andrews. (1999). The human embryonal carcinoma marker antigen TRA-1-60 is a sialylated keratan sulfate proteoglycan. *Cancer Res* 59:4715–4719.
- Brimble SN, ES Sherrer, EW Uhl, E Wang, S Kelly, AH Merrill Jr., AJ Robins and TC Schulz. (2007). The cell surface glycosphingolipids SSEA-3 and SSEA-4 are not essential for human ESC pluripotency. *Stem Cells* 25:54–62.
- Przyborski SA. (2001). Isolation of human embryonal carcinoma stem cells by immunomagnetic sorting. *Stem Cells* 19:500–504.
- Sidhu KS and BE Tuch. (2006). Derivation of three clones from human embryonic stem cell lines by FACS sorting and their characterization. *Stem Cells Dev* 15:61–69.
- Ferrandina G, G Bonanno, L Pierelli, A Perillo, A Procoli, A Mariotti, M Corallo, E Martinelli, S Rutella, A Paglia, G Zannoni, S Mancuso and G Scambia. (2007). Expression of CD133-1 and CD133-2 in ovarian cancer. *Int J Gynecol Cancer* 18:506–514.
- Ferrandina G, E Martinelli, M Petrillo, MG Prisco, G Zannoni, S Sioletic and G Scambia. (2009). CD133 antigen expression in ovarian cancer. *BMC Cancer* 9:221–229.
- Kusumbe AP, AM Mali and SA Bapat. (2009). CD133-expressing stem cells associated with ovarian metastases establish an endothelial hierarchy and contribute to tumor vasculature. *Stem Cells* 27:498–508.
- Bonfanti L. (2006). PSA-NCAM in mammalian structural plasticity and neurogenesis. *Prog Neurobiol* 80:129–164.
- Gascon E, L Vutskits and JZ Kiss. (2007). Polysialic acid-neural cell adhesion molecule in brain plasticity: from synapses to integration of new neurons. *Brain Res Rev* 56:101–118.
- Plaia TW, R Josephson, Y Liu, X Zeng, C Ording, A Toumadje, SN Brimble, ES Sherrer, EW Uhl, WJ Freed, TC Schulz, A Maitra, MS Rao and JM Auerbach. (2006). Characterization of a new NIH-registered variant human embryonic stem cell line, BG01V: a tool for human embryonic stem cell research. *Stem Cells* 24:531–546.
- Wang L, TC Schulz, ES Sherrer, DS Dauphin, S Shin, AM Nelson, CB Ware, M Zhan, CZ Song, X Chen, SN Brimble, A McLean, MJ Galeano, EW Uhl, KA D'Amour, JD Chesnut, MS Rao, CA Blau and AJ Robins. (2007). Self-renewal of human embryonic stem cells requires insulin-like growth factor-1 receptor and ERBB2 receptor signaling. *Blood* 110:4111–4119.
- Harlow E and D Lane. (1998). *Using Antibodies. A Laboratory Manual*. Cold Spring Harbor Laboratory Press, Cold Spring Harbor, NY, p 495.
- Price PW, EC McKinney, Y Wang, LE Sasser, MK Kandasamy, L Matsuuchi, C Milcarek, RB Deal, DG Culver and RB Meagher. (2009). Engineered cell surface expression of membrane immunoglobulin as a means to identify monoclonal antibody-secreting hybridomas. *J Immunol Methods* 343:28–41.
- Gildersleeve JC, O Oyelaran, JT Simpson and B Allred. (2008). Improved procedure for direct coupling of carbohydrates to proteins via reductive amination. *Bioconjugate Chem* 19:1485–1490.
- Oyelaran OO, Q Li, DF Farnsworth and JC Gildersleeve. (2009). Microarrays with varying carbohydrate density reveal distinct subpopulations of serum antibodies. *J Proteome Res* 8:3529–3538.
- Oyelaran O, LM McShane, L Dodd and JC Gildersleeve. (2009). Profiling human serum antibodies with a carbohydrate antigen microarray. *J Proteome Res* 8:4301–4310.
- Song EH and NLB Pohl. (2009). Carbohydrate arrays: recent developments in fabrication and detection methods with applications. *Curr Opin Chem Biol* 13:626–632.
- Oyelaran O and JC Gildersleeve. (2009). Glycan arrays: recent advances and future challenges. *Curr Opin Chem Biol* 13:406–413.
- Liu Y, AS Palma and T Feizi. (2009). Carbohydrate microarrays: key developments in glycobiology. *Biol Chem* 390:647–656.

23. Jones RB, A Gordus, JA Krall and G MacBeath. (2006). A quantitative protein interaction network for the ErbB receptors using protein microarrays. *Nature* 439:168–174.
24. Kobata A and V Ginsburg. (1972). Oligosaccharides of human milk. 3. Isolation and characterization of a new hexasaccharide, lacto-N-hexaose. *J Biol Chem* 247:1525–1529.
25. Yamashita K, Y Tachibana and A Kobata. (1977). Oligosaccharides of human milk: structures of three lacto-N-hexaose derivatives with H-haptenic structure. *Arch Biochem Biophys* 182:546–555.
26. Dua VK, K Goso, VE Dube and CA Bush. (1985). Characterization of lacto-N-hexaose and two fucosylated derivatives from human milk by high-performance liquid chromatography and proton NMR spectroscopy. *J Chromatogr* 328:259–269.
27. Loo D, N Pryer, P Young, T Liang, S Coberly, KL King, K Kang, P Roberts, M Tsao, X Xu, B Potts and JP Mather. (2007). The glycotope-specific RAV12 monoclonal antibody induces oncosis in vitro and has antitumor activity against gastrointestinal adenocarcinoma tumor xenografts in vivo. *Mol Cancer Ther* 6:856–865.
28. Coberly SK, FZ Chen, MP Armanini, Y Chen, PF Young, JP Mather and DT Loo. (2009). The RAV12 monoclonal antibody recognizes the N-linked glycotope RAAG12: expression in human normal and tumor tissues. *Arch Pathol Lab Med* 133:1403–1412.
29. Rettig WJ, C Cordon-Cardo, JS Ng, HF Oettgen, LJ Old and KO Lloyd. (1985). High-molecular-weight glycoproteins of human teratocarcinoma defined by monoclonal antibodies to carbohydrate determinants. *Cancer Res* 45:815–821.
30. Gooi HC, LK Williams, K Uemura, EF Hounsell, RA McIlhinney and Feizi T. (1983). A marker of human foetal endoderm defined by a monoclonal antibody involves type 1 blood group chains. *Mol Immunol* 20:607–613.
31. Williams LK, A Sullivan, RA McIlhinney and AM Neville. (1982). A monoclonal antibody marker of human primitive endoderm. *Int J Cancer* 30:731–738.
32. Ohbayashi H, T Endo, K Yamashita, M Kuroki, Y Matsuoka and A Kobata. (1989). Novel methods to determine the epitopes on the asparagine-linked oligosaccharides of glycoproteins. *Anal Biochem* 182:200–206.
33. Kabat EA, J Liao, J Shyong and EF Osserman. (1982). A monoclonal IgM lambda macroglobulin with specificity for lacto-N-tetraose in a patient with bronchogenic carcinoma. *J Immunol* 128:540–544.
34. Nozawa S, S Narisawa, K Kojima, M Sakayori, R Iizuka, H Mochizuki, T Yamauchi, M Iwamori and Nagai Y. (1989). Human monoclonal antibody (HMST-1) against lacto-series type 1 chain and expression of the chain in uterine endometrial cancers. *Cancer Res* 49:6401–6406.
35. Lanctot PA, FH Gage and AP Varki. (2007). The glycans of stem cells. *Curr Opin Chem Biol* 11:373–380.
36. Heiskanen A, T Hirvonen, H Salo, U Impola, A Olonen, A Laitinen, S Tiitinen, S Natunen, O Aitio, H Miller-Podraza, M Wuhrer, AM Deelder, J Natunen, J Laine, P Lehenkari, J Saarinen, T Satomaa and L Valmu. (2009). Glycomics of bone marrow-derived mesenchymal stem cells can be used to evaluate their cellular differentiation stage. *Glycoconj J* 26:367–384.
37. Satomaa T, A Heiskanen, M Mikkola, C Olsson, M Blomqvist, M Tiittanen, T Jaatinen, O Aitio, A Olonen, J Helin, J Hiltunen, J Natunen, T Tuuri, T Otonkoski, J Saarinen and J Laine. (2009). The N-glycome of human embryonic stem cells. *BMC Cell Biol* 2:10:42.
38. Sell S. (2004). Stem cell origin of cancer and differentiation therapy. *Crit Rev Oncol Hematol* 51:1–28.
39. Soltysova A, V Altanarova and C Altaner. (2005). Cancer stem cells. *Neoplasma* 52:435–440.
40. Martinez-Clement JA, EJ Andreu and F Prosper. (2006). Somatic stem cells and the origin of cancer. *Clin Transl Oncol* 8:647–663.
41. Bertolini G, L Roz, P Perego, M Tortoreto, E Fontanella, L Gatti, G Pratesi, A Fabbri, F Andriani, S Tinelli, E Roz, R Caserini, Lo S Vullo, T Camerini, L Mariani, D Delia, E Calabrò, U Pastorino and G Sozzi. (2009). Highly tumorigenic lung cancer CD133+ cells display stem-like features and are spared by cisplatin treatment. *Proc Natl Acad Sci U S A* 106:16281–16286.
42. Buess M, M Rajsiki, BML Vogel-Durrer, R Herrmann and C Rochlitz. (2009). Tumor-endothelial interaction links the CD44+/CD24– phenotype with poor prognosis in early-stage breast cancer. *Neoplasia* 11:987–1002.
43. Singh S, ID Clarke, T Hide and PB Dirks. (2004). Cancer stem cells in nervous system tumors. *Oncogene* 23:7267–7273.
44. Bidlingmaier S, X Zhu and B Liu. (2008). The utility and limitations of glycosylated human CD133 epitopes in defining cancer stem cells. *J Mol Med* 86:1025–1032.
45. Wright MH, AM Calcagno, CD Salcido, MD Carlson, SV Ambudkar and L Varticovski. (2008). Brca1 breast tumors contain distinct CD44+/CD24– and CD133+ cells with cancer stem cell characteristics. *Breast Cancer Res* 10:R10.
46. Yang RY, GA Rabinovich and FT Liu. (2008). Galectins: structure, function and therapeutic potential. *Expert Rev Mol Med* 10:e17.
47. Rabinovich GA and MA Toscano. (2009). Turning “sweet” on immunity: galectin-glycan interactions in immune tolerance and inflammation. *Nat Rev Immunol* 9:338–352.
48. Consortium for Functional Glycomics (CFG). Available at: www.functionalglycomics.org/glycomics/publicdata/primaryscreen.jsp
49. Saussez S, C Decaestecker, S Cludts, P Ernoux, D Chevalier, Smetana K Jr., S André, X Leroy and HJ Gabius. (2009). Adhesion/growth-regulatory tissue lectin galectin-1 in relation to angiogenesis/lymphocyte infiltration and prognostic relevance of stromal up-regulation in laryngeal carcinomas. *Anticancer Res* 29:59–65.
50. Chan J, K O’Donoghue, M Gavina, Y Torrente, N Kennea, H Mehmet, H Stewart, DJ Watt, JE Morgan and NM Fisk. (2006). Galectin-1 induces skeletal muscle differentiation in human fetal mesenchymal stem cells and increases muscle regeneration. *Stem Cells* 24:1879–1891.
51. Sakaguchi M, T Shingo, T Shimazaki, HJ Okano, M Shiwa, S Ishibashi, H Oguro, M Ninomiya, T Kadoya, H Horie, A Shibuya, H Mizusawa, F Poirier, H Nakauchi, K Sawamoto and H Okano. (2006). A carbohydrate-binding protein, galectin-1, promotes proliferation of adult neural stem cells. *Proc Natl Acad Sci U S A* 103:7112–7117.
52. Lee MY, SH Lee, JH Park and HJ Han. (2009). Interaction of galectin-1 with caveolae induces mouse embryonic stem cell proliferation through the Src, ERas, Akt and mTOR signaling pathways. *Cell Mol Life Sci* 66:1467–1478.
53. Vas V, R Fajka-Boja, G Ion, V Dudics, E Monostori and F Uher. (2005). Biphasic effect of recombinant galectin-1 on the growth and death of early hematopoietic cells. *Stem Cells* 23:279–287.

54. Garner OB and LG Baum. (2008). Galectin-glycan lattices regulate cell-surface glycoprotein organization and signaling. *Biochem Soc Trans* 36(Pt 6):1472–1477.
55. Friedrichs J, A Manninen, DJ Muller and J Helenius. (2008). Galectin-3 regulates integrin alpha2beta1-mediated adhesion to collagen-I and -IV. *J Biol Chem* 283:32264–32272.
56. Saravanan C, FT Liu, IK Gipson and N Panjwani. (2009). Galectin-3 promotes lamellipodia formation in epithelial cells by interacting with complex N-glycans on alpha3beta1 integrin. *J Cell Sci* 15:122(Pt20):3684–3693.
57. Nakahara S and A Raz. (2008). Biological modulation by lectins and their ligands in tumor progression and metastasis. *Anticancer Agents Med Chem* 8:22–36.
58. Saussez S and R Kiss. (2006). Galectin-7. *Cell Mol Life Sci* 63:686–697.
59. Lajoie P, JG Goetz, JW Dennis and IR Nabi. (2009). Lattices, rafts, and scaffolds: domain regulation of receptor signaling at the plasma membrane. *J Cell Biol* 185:381–385.

Address correspondence to:

*Mohamed G. Shoreibah, Director of R&D
Abeome Corporation
111 Riverbend Road
Athens, GA 3060518*

E-mail: mohamed.shoreibah@abeomecorp.com

Received for publication April 28, 2010

Accepted after revision October 1, 2010

Prepublished on Liebert Instant Online October 1, 2010

